Supplement of Atmos. Chem. Phys., 25, 3841–3856, 2025
https://doi.org/10.5194/acp-25-3841-2025-supplement

Atmospheric Chemistry and Physics
Open Access
EGU

Supplement of

Pristine oceans are a significant source of uncertainty in quantifying global cloud condensation nuclei

Goutam Choudhury et al.

Correspondence to: Goutam Choudhury (goutam.choudhury@biu.ac.il)

Content:

Supplementary Figures S1 to S11

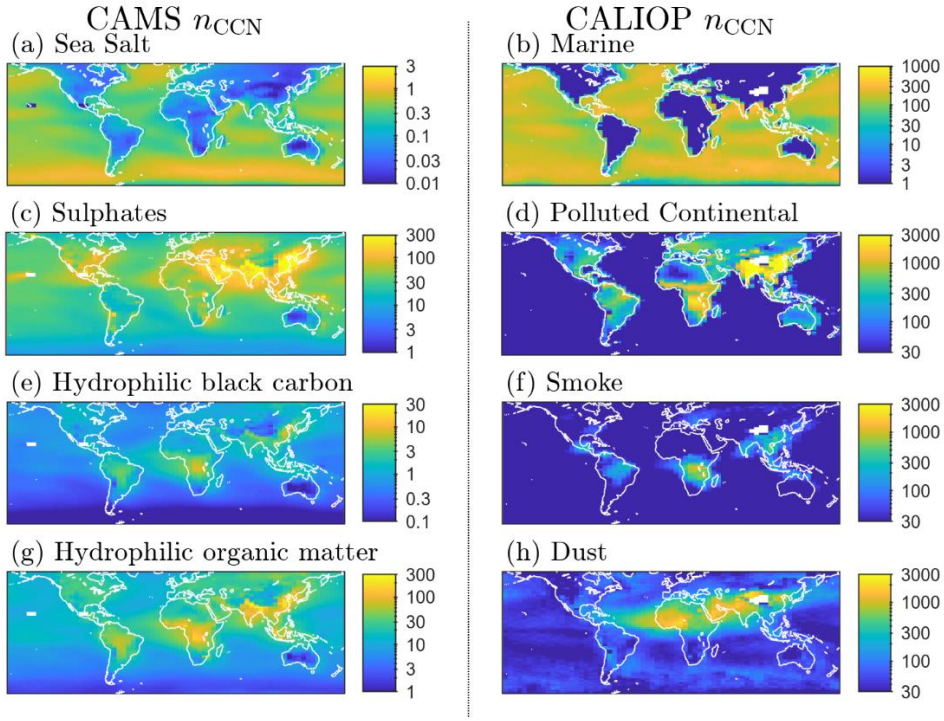

Figure S1: Global map of aerosol-type-specific climatology of cloud condensation nuclei concentrations (n_{CCN}) derived from CAMS (left column) and CALIOP (right column) datasets. Data from June 2006 through December 2021 are used to generate the average global maps.

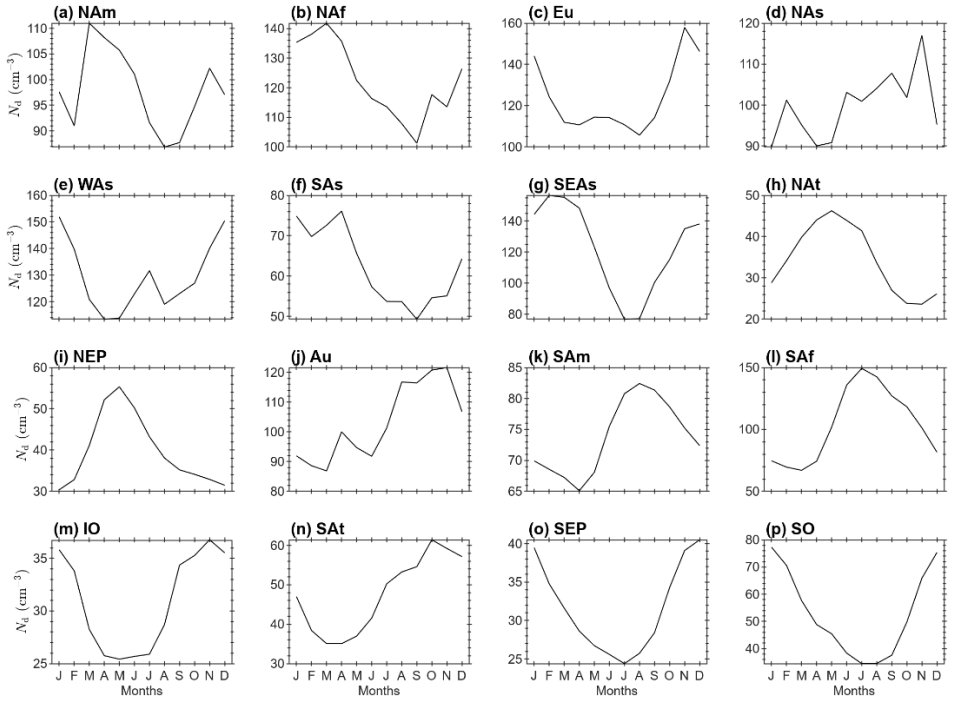

Figure S2: Monthly variations in cloud droplet number concentrations (N_d) for various regions. Panels (a) to (i) correspond to Northern Hemisphere regions, while panels (j) to (p) represent Southern Hemisphere regions. Datasets from June 2006 through December 2020 are used to generate the monthly climatology.

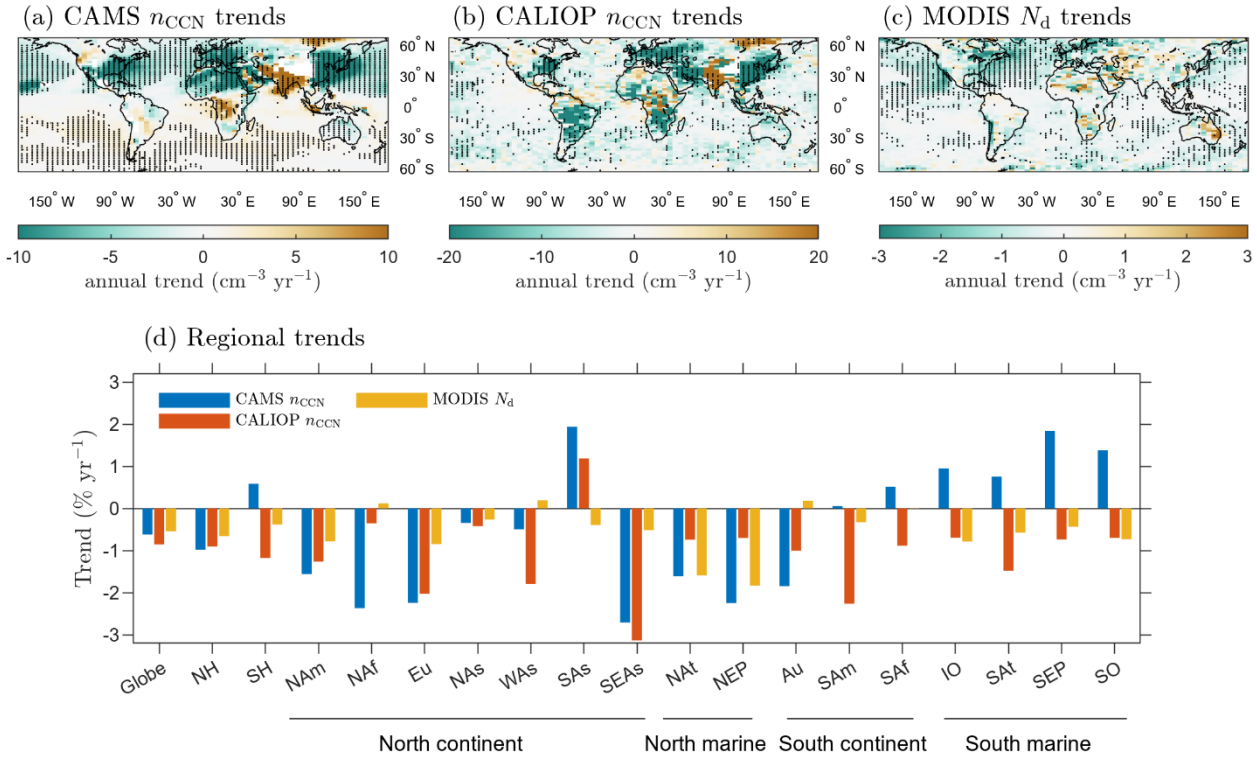

Figure S3: Same as Fig. 5 in the manuscript but in units of cm^{-3}yr^{-1} for panels (a), (b), and (c) and in % yr^{-1} for panel (d).

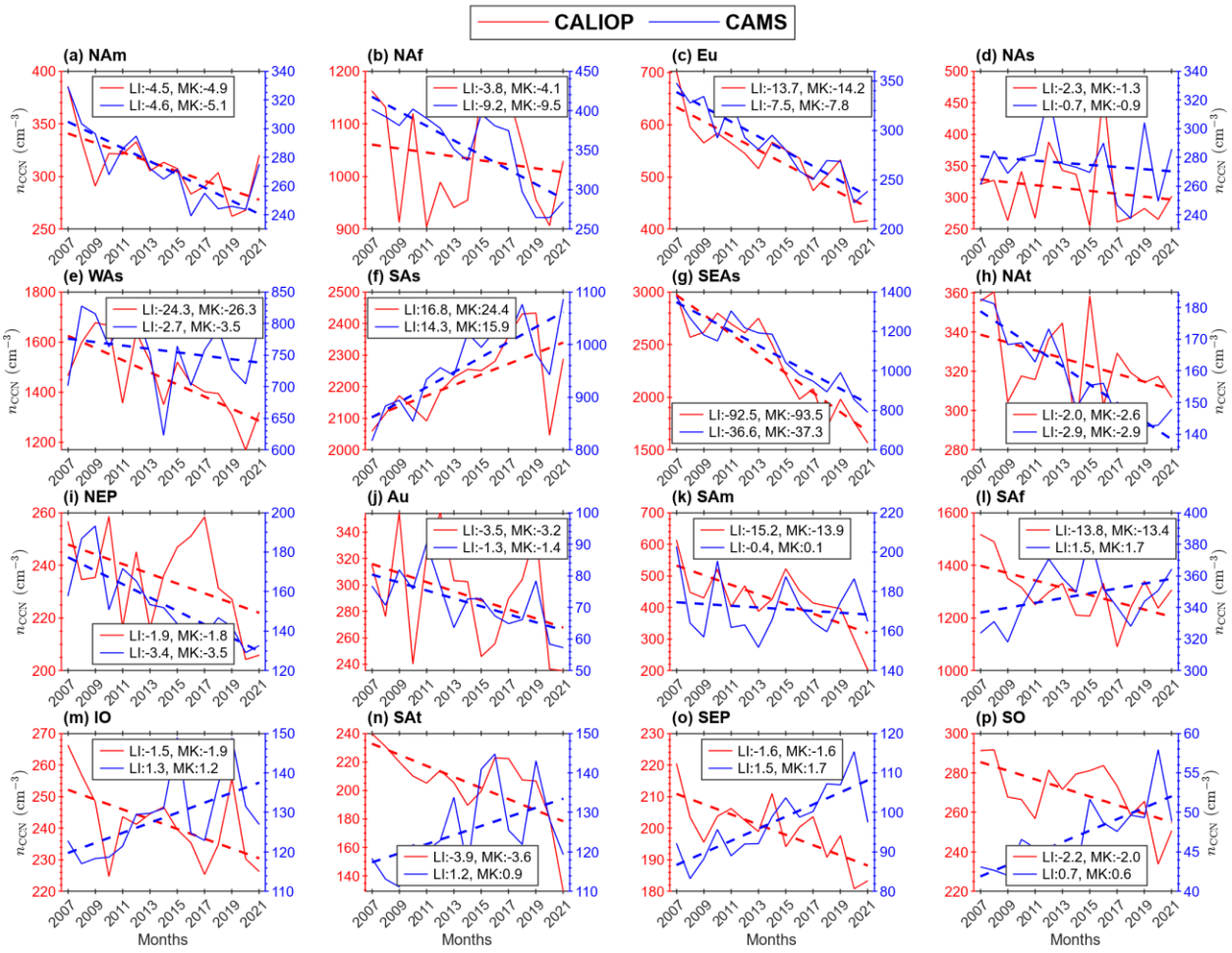

Figure S4: Annual time series of cloud condensation nuclei concentrations (n_{CCN}) derived from CALIOP (in red) and CAMS (in blue) for 16 regional domains considered in the study. LI and MK in the legend of each panel represent the linear slope and Mann-Kendal slope, respectively.

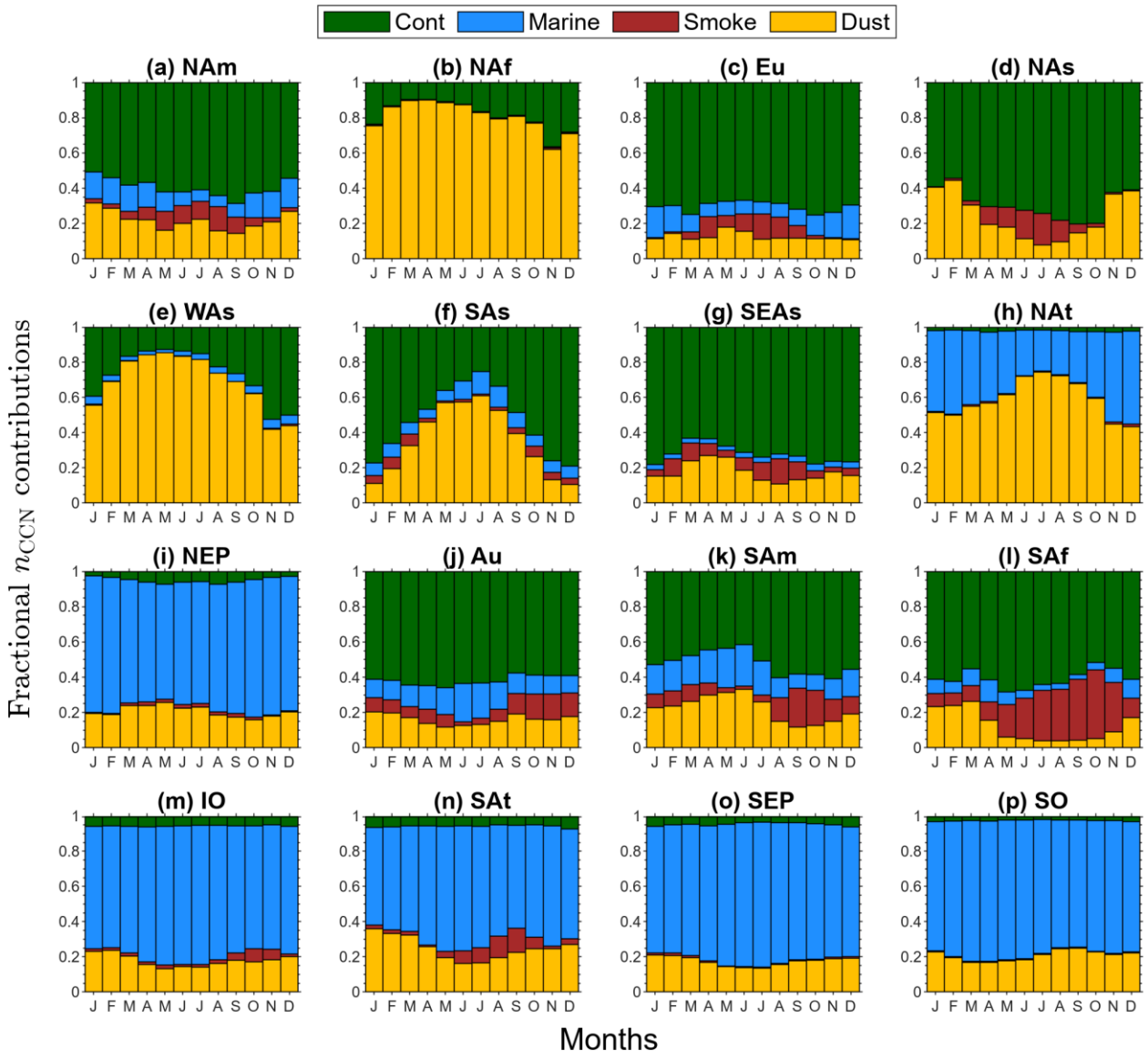

Figure S5: Extended Fig. A1 of the manuscript showing fractional contributions of different aerosol species to the total cloud condensation nuclei concentrations (n_{CCN}) for all regional domains considered in the study.

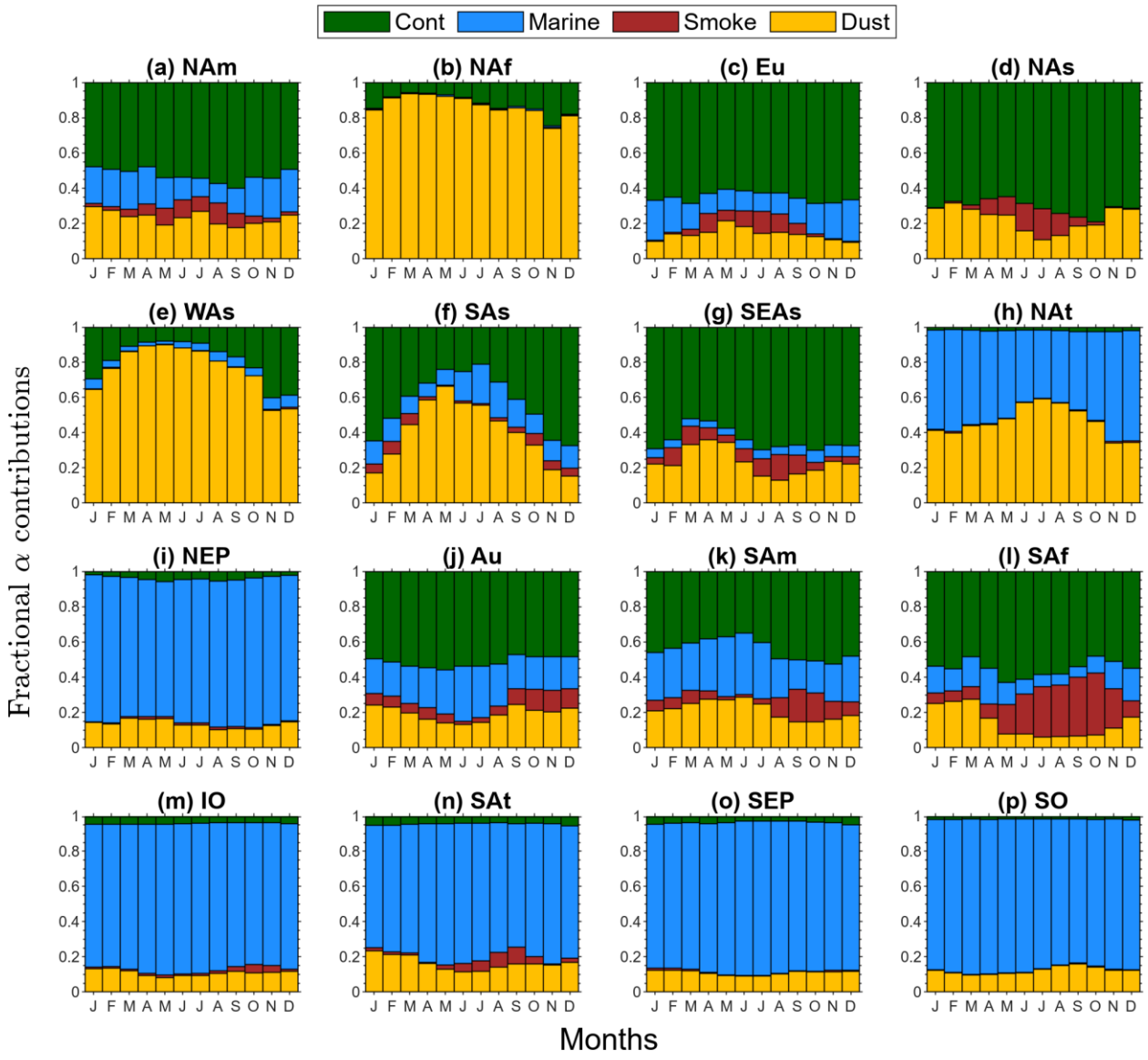

Figure S6: Same as Fig. S4 but for extinction coefficients (α) instead of cloud condensation nuclei concentrations (n_{CCN}). The figure is an extension of Fig. A1 in the manuscript.

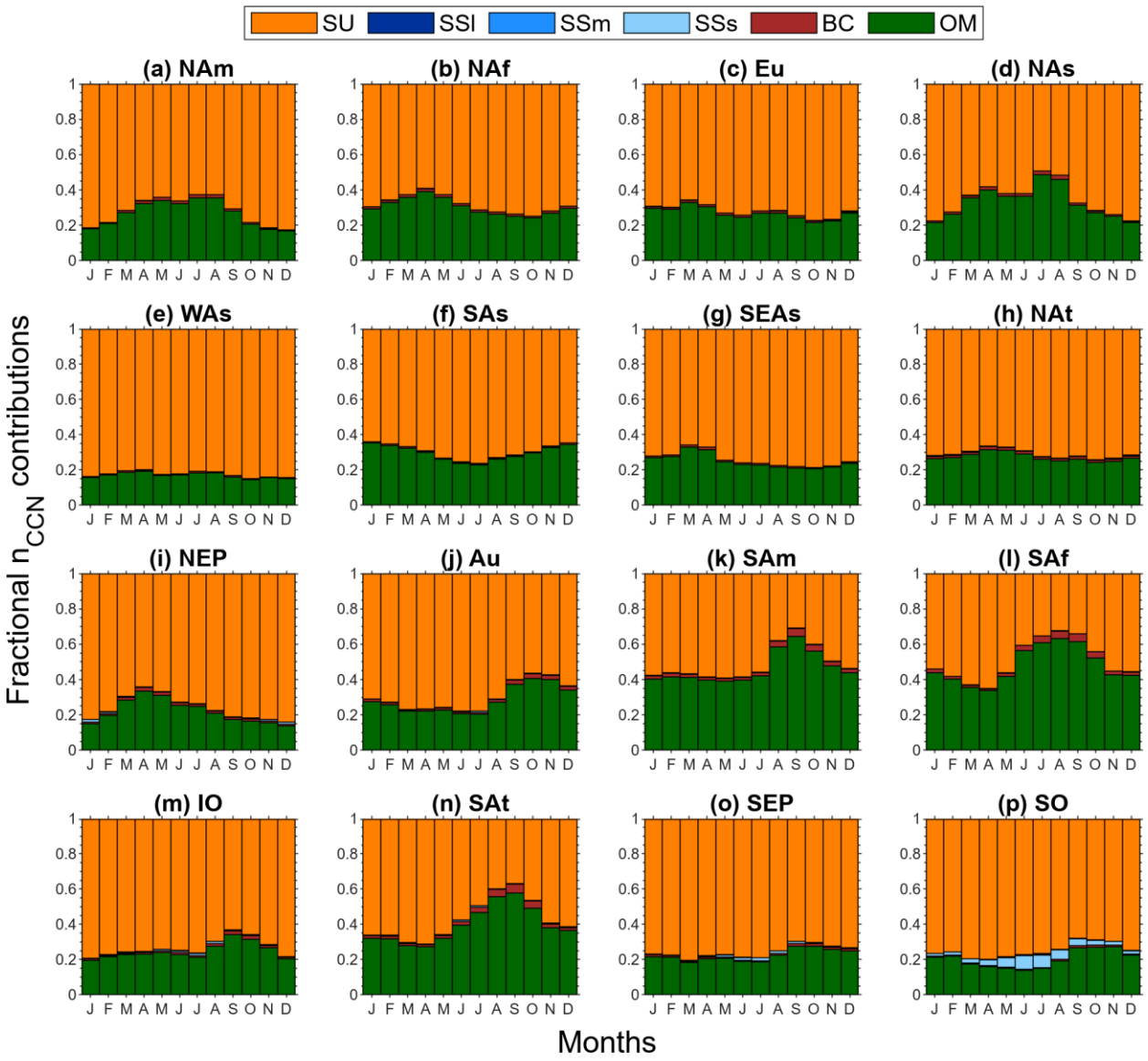

Figure S7: Same as Fig. S4, but for CAMS retrievals of cloud condensation nuclei concentrations (n_{CCN}). The figure is an extension of Fig. A1 in the manuscript.

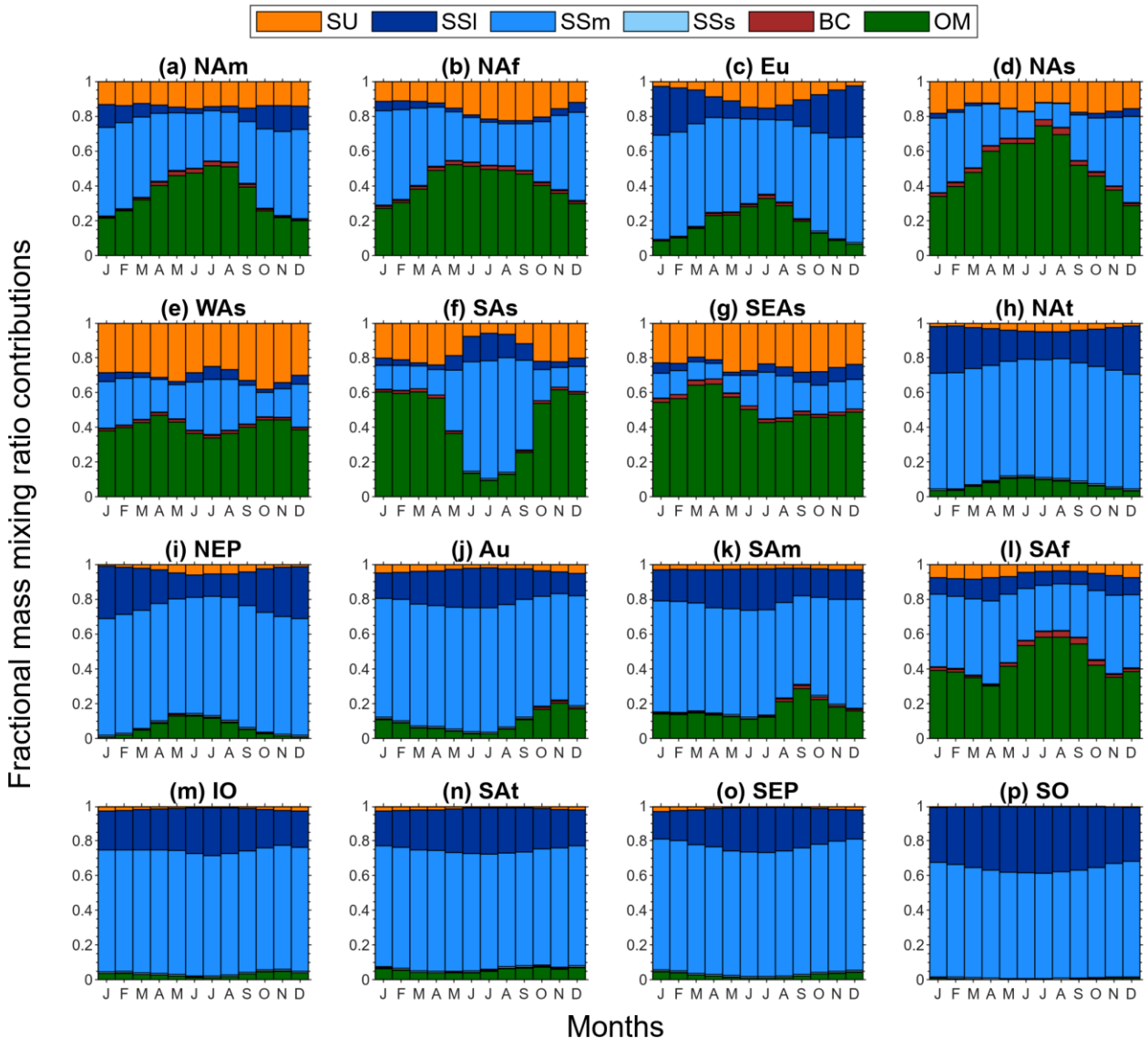

Figure S8: Same as Fig. S6, but for mass mixing ratio (MMR) instead of cloud condensation nuclei concentrations (n_{CCN}). The figure is an extension of Fig. A1 in the manuscript.

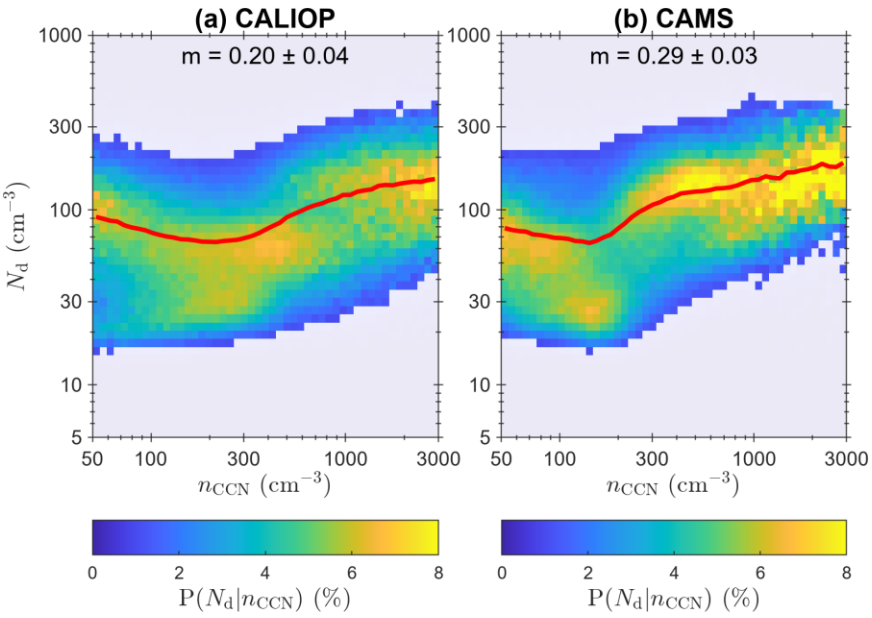

Figure S9: Global aggregated joint histograms depicting the conditional probability of occurrence of N_d for a given n_{CCN}. m represents the N_d-n_{CCN} susceptibility term estimated as the slope of the linear regression to the mean N_d (red line) for every n_{CCN} interval. Monthly N_d and n_{CCN} datasets from June 2006 through December 2020 are used.

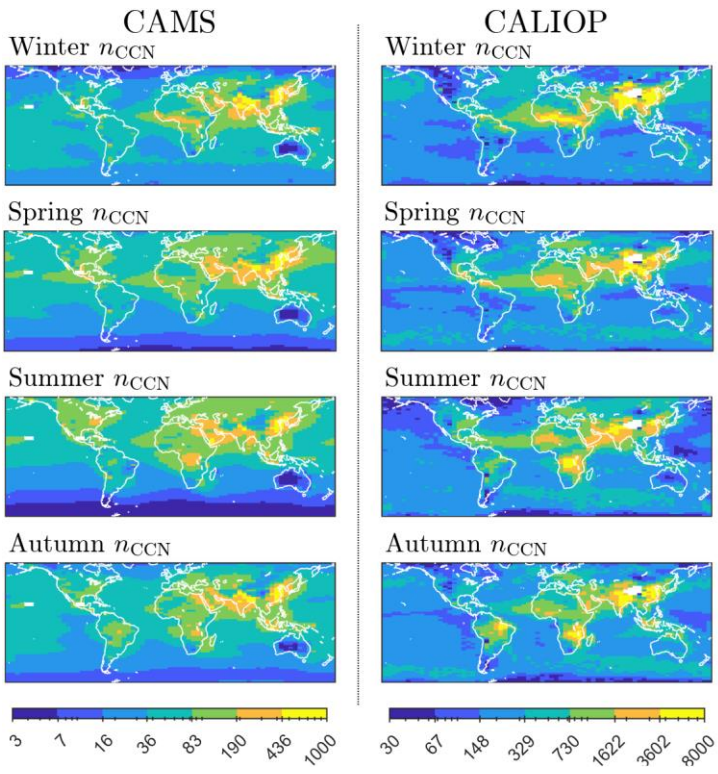

Figure S10: Seasonal climatology of cloud condensation nuclei concentrations (n_{CCN}) derived from CAMS (left column) and CALIOP (right column).

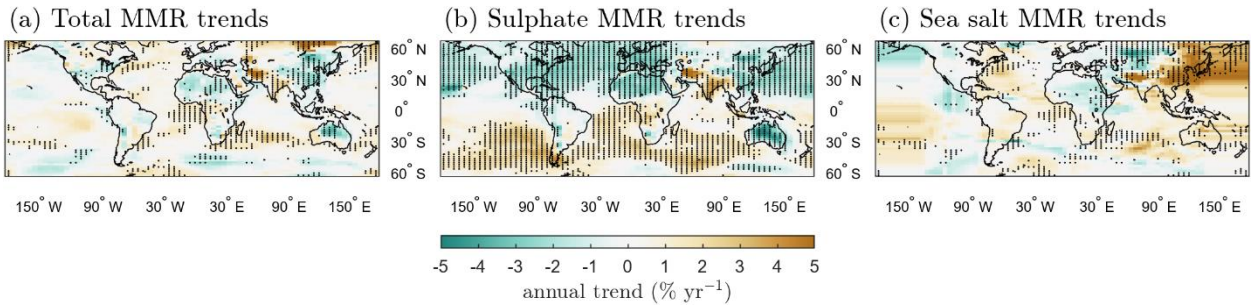

Figure S11: Annual trends in % yr^{-1} derived from CAMS's (a) total aerosol mass mixing ratio (MMR), (b) sulphate mass mixing ratio, and (c) sea salt mass mixing ratio.